

# Time-dependent density functional theory for strong-field ionization by circularly polarized pulses

Ciprian C. Chirilă<sup>1</sup>, Manfred Lein<sup>2</sup>

<sup>1</sup> Institute of High Performance Computing, Agency for Science, Technology and Research, 1 Fusionopolis Way #16-16 Connexis, Singapore 138632, Republic of Singapore

<sup>2</sup> Institut für Theoretische Physik and Centre for Quantum Engineering and Space-Time Research (QUEST), Leibniz Universität Hannover, Appelstraße 2, 30167 Hannover, Germany

**Abstract.** By applying time-dependent density functional theory to a two-dimensional multielectron atom subject to strong circularly polarized light pulses, we confirm that the ionization of  $p$  orbitals with defined angular momentum depends on the sense of rotation of the applied field. A simple ad-hoc modification of the adiabatic local-density exchange-correlation functional is proposed to remedy its unphysical behaviour under orbital depletion.

*Keywords:* time-dependent density functional theory, strong-field ionization

## 1. Introduction

The dynamics of atoms and molecules in strong laser pulses is of immense interest as it is the basis of current realizations of attosecond-scale experiments [1]. More specifically, photoelectron momentum distributions from ionization by circularly polarized pulses have found a number of important applications such as molecular imaging [2–6] and the subcycle investigation of atomic tunnel ionization dynamics using the attoclock method [7–9]. In chemistry, multiphoton photoelectron circular dichroism in the momentum distributions from ionization of chiral molecules is a new tool for chiral recognition [10–15].

In general, the theory of nonperturbative strong-field ionization is a challenge due to the simultaneous action of the laser and Coulomb forces, including electron-electron interaction for multielectron systems. For atoms treated in a single-active-electron approximation, however, many beautiful results have been obtained in Keldysh-type theories, see [16] and references therein. One fundamental result concerning circular polarization is the different ionization rate of atomic  $p_+$  and  $p_-$  orbitals in a field of given sense of rotation, where  $p_+$  and  $p_-$  denote  $p$  orbitals (orbital angular momentum  $l = 1$ ) with defined magnetic quantum numbers  $m = +1$  and  $m = -1$ , respectively

[17, 18]. According to the theory, counter-rotating electrons, i.e. with sense of rotation opposite to the electric field of the applied laser pulse, are freed more easily than co-rotating electrons. This prediction has been essentially verified in numerical solutions of the time-dependent Schrödinger equation for a two-dimensional atom in the single-active-electron approximation [19]. We mention that for sufficiently long wavelengths and high field strengths, however, the numerical results have shown a different behaviour arising from the dressing of the orbitals prior to ionization [19, 20]. In practice, strong-field ionization experiments are often carried out with rare-gas atoms where  $p_+$  and  $p_-$  orbitals are equally occupied in the closed shell of the atomic ground state. Thus, the experimental verification of the predicted effects is not trivial. In an experiment where argon atoms were doubly ionized by a sequence of two time-delayed circular pulses with either equal or opposite helicities, the effect could be observed [21, 22].

The theoretical description of atomic ionization processes requires in principle the proper treatment of many interacting electrons. However, the time-consuming direct numerical solution of the time-dependent Schrödinger equation is not an option for electron numbers larger than two or three [23, 24]. A well known alternative is provided by the time-dependent density functional theory (TDDFT) [25, 26]. It replaces the many-body Schrödinger equation by a set of single-electron Schrödinger equations, known as Kohn-Sham (KS) equations, determining the time evolution of single-particle orbitals in an effective KS potential. The KS potential is, in principle, chosen such that the total electron density of the Kohn-Sham system reproduces the density of the interacting multielectron system. In practice, the KS potential is implemented by using one of the approximations available in the literature. Unfortunately, standard approximations such as the local-density approximation (LDA) suffer from severe deficiencies when applied to strong-field ionization. In particular, the substantial signal of nonsequential double ionization of rare-gas atoms at low laser intensities, leading to a “knee structure” in the intensity dependence of the double-ionization yield [27, 28], could not be theoretically reproduced by such an approach [29–31]. Even the single-ionization yield is substantially underestimated by the naive TDDFT approach. It has been realized that these failures are due to the fact that the standard approximations do not incorporate the correct dependence on the number of bound electrons, which changes during the ionization process [32]. It is known already from static density functional theory that the KS potential for fractional particle numbers possesses a discontinuity when the particle number passes through an integer [33]. Simple approximations such as a time-dependent Hartree method or LDA depend instead smoothly on the particle number. Thus they cannot handle, for example, situations where ionization has removed nearly one electron. In [32] it was shown that the results can be improved by including a quasidiscontinuous behaviour by hand, leading to a knee structure in the double ionization yield and to an increased single-ionization yield. Systematic approaches to construct approximations respecting the discontinuity have been proposed, but have not yet found wide-spread application in strong-field ionization [34–36]. It should be noted that the calculation of the single- and double-ionization yields from the density

is a further issue in TDDFT, which we do not address in depth in the present paper. For two-electron systems, an adiabatic approach was shown to work well [37]. For many-electron systems, however, there does not seem to be an easy-to-implement way to go beyond the “mean-field” approximation which obtains the ionization probabilities directly from the KS wave function constructed from KS orbitals despite the fact that TDDFT does not directly ascribe physical meaning to the KS orbitals.

In the present work, we demonstrate the application of TDDFT to strong-field ionization by circularly polarized laser pulses. Since the nonperturbative numerical treatment of circular polarization is time-consuming even for one-electron calculations, we restrict ourselves to a two-dimensional (2D) model atom. Our work can therefore be viewed as a multielectron generalization of the 2D single-active-electron calculation reported in [19]. To avoid the known issue of underestimated ionization probabilities we propose and employ a multielectron version of the ad hoc correction of the KS potential used in [32]. Essentially our multielectron calculation confirms the  $m$ -dependence of the orbital ionization rate. We demonstrate also the application to double-pulse irradiation following the experimental scheme of [21]. However, due to a lack of reliable functionals for calculating the double-ionization probability in a multielectron system, we are currently not able to reproduce the experimental results. Atomic units are used throughout this paper.

## 2. Theory

We consider a 2D model atom with potential

$$v_0(\mathbf{r}) = -\frac{6}{\sqrt{0.1 + \mathbf{r}^2}} \quad (1)$$

filled with 6 electrons. In the ground state, the system is spin saturated so that for each spin projection ( $\uparrow$  and  $\downarrow$ ) there are three occupied orbitals. The charge  $Z=6$  is chosen to obtain a configuration where the degenerate highest occupied orbitals with magnetic quantum numbers  $m=-1$  and  $m=+1$  are fully occupied. We refer to these orbitals as  $p_-$  and  $p_+$ . Their KS eigenvalue, -0.21 a.u. is identified with the first ionization potential of the model atom. The lowest orbital has zero angular momentum ( $s$  orbital). This model atom can be viewed as the 2D analog to a three-dimensional rare-gas atom.

The time-dependent KS orbitals  $\varphi_j(\mathbf{r}, t)$  satisfy the KS equations

$$i\frac{\partial\varphi_j(\mathbf{r}, t)}{\partial t} = \left(-\frac{\nabla^2}{2} + v_s(\mathbf{r}, t)\right)\varphi_j(\mathbf{r}, t) \quad (2)$$

where the spin index is omitted because both spin projections have the same orbitals. When the system is subject to laser irradiation treated in the dipole approximation, the KS potential consists of the external potential  $v_0 + \mathbf{r} \cdot \mathbf{E}(t)$  with electric field  $\mathbf{E}(t)$ , the Hartree potential  $v_h$  and the exchange-correlation potential  $v_{xc}$ ,

$$v_s(\mathbf{r}, t) = v_0(\mathbf{r}, t) + \mathbf{r} \cdot \mathbf{E}(t) + v_h[n](\mathbf{r}, t) + v_{xc}[n](\mathbf{r}, t). \quad (3)$$

The latter two quantities are functionals of the density  $n$ ,

$$n(\mathbf{r}, t) = 2 \sum_{j=1,2,3} |\varphi_j(\mathbf{r}, t)|^2. \quad (4)$$

Specifically, the Hartree potential is

$$v_h[n](\mathbf{r}, t) = \int \frac{n(\mathbf{r}', t)}{|\mathbf{r} - \mathbf{r}'|} d^2r'. \quad (5)$$

For the exchange-correlation potential, we resort to the adiabatic LDA potential  $v_{xc}^{\text{LDA}}$  based on the 2D homogeneous electron gas, using the parametrization given in [38]. As indicated in the introduction, however, the performance of plain LDA for strong-field ionization processes is poor as it misses effects related to the particle-number discontinuity. In the same spirit as in [32], we therefore introduce an ad hoc correction factor that multiplies the Hartree-exchange-correlation potential. Thus, in this modified version of the numerical simulation, we use

$$v_s(\mathbf{r}, t) = v_0(\mathbf{r}, t) + \mathbf{r} \cdot \mathbf{E}(t) + c(N(t)) \left( v_h[n](\mathbf{r}, t) + v_{xc}^{\text{LDA}}[n](\mathbf{r}, t) \right). \quad (6)$$

Here, the argument  $N(t)$  of the correction factor  $c$  is the number of bound electrons at time  $t$ , which is obtained by integrating the electron density over a small region around the nucleus. In our 2D simulation, this region is a square with edges from -5 a.u. to +5 a.u. The function  $c(N)$  is constructed as follows. Its purpose is to compensate for the loss of bound electrons due to ionization. The main idea is an adiabatic ionization process in the sense that the remaining ion is created in its ground state. At integer  $N$ , we require that  $c \approx 1$ , based on the assumption that the exchange-correlation functional  $v_{xc}^{\text{LDA}}[n]$  is a good approximation for integer particle numbers. For decreasing  $N$ , the (uncorrected) Hartree-exchange-correlation potential decreases and we assume that it is roughly proportional to  $N$ . To compensate this behaviour and thus to maintain the overall “strength” of the Hartree-exchange-correlation potential until the next integer particle number is reached, we demand that  $c \approx N_{\text{int}}/N$  where  $N_{\text{int}}$  is the next higher integer number above  $N$ . For  $N < 1$ , there is no electron-electron interaction in the bound state. We therefore demand  $c \approx 0$  for  $N < 1$ . For the 6-electron system, all the above requirements are met by the function

$$c(N) = \frac{6}{N} \frac{1}{1 + e^{100(\frac{6}{N} - \frac{6}{5})}} + \sum_{j=2}^5 \frac{j}{N} \frac{1}{1 + e^{100(\frac{j+1}{j} - \frac{j+1}{N})} + e^{100(\frac{j}{N} - \frac{j}{j-1})}}. \quad (7)$$

The number 100 in the exponents is arbitrarily chosen to achieve a sufficiently fast change of the function in the vicinity of integer arguments. The shape of the function  $c(N)$  is shown in figure 1. Calculations according to equations (6),(7) are labelled as modified LDA (mLDA) in the following.

We study the dynamics in circularly polarized fields of the form  $\mathbf{E}_{\pm}(t) = -d\mathbf{A}_{\pm}(t)/dt$  with

$$\mathbf{A}_{\pm}(t) = -\frac{\mathcal{E}}{\omega} s(t) [\sin(\omega t)\mathbf{e}_x \mp \cos(\omega t)\mathbf{e}_y] \quad (8)$$

where  $\omega$  is the laser frequency,  $\mathcal{E}$  is the field amplitude and  $s(t)$  is the field envelope. We will mostly use a very short  $\sin^2$ -shaped envelope with a duration of three optical

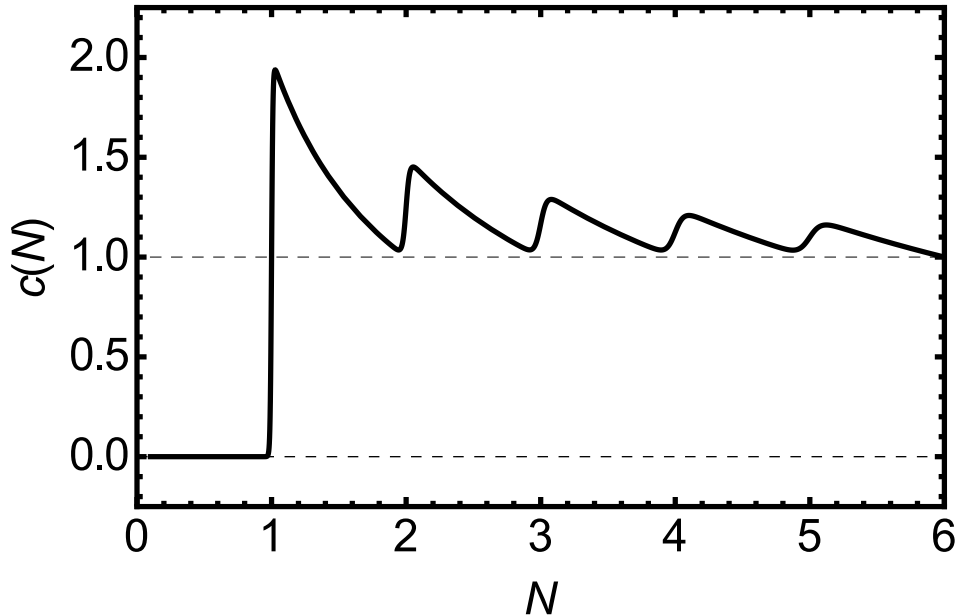


**Figure 1.** The correction  $c(N)$  is used as a prefactor of the Hartree-exchange-correlation potential in the mLDA method. This plot shows  $c(N)$  versus the number  $N$  of bound electrons.

cycles (see [19] where the same pulse form was used). The  $\pm$  sign determines the sense of field rotation. In the following we refer to  $\mathbf{E}_+$  as right-circularly polarized field and  $\mathbf{E}_-$  as left-circularly polarized field.

The orbitals are represented on a grid in real space with spacing  $\Delta_x = \Delta_y = 0.15$  and 666 points in each direction. The time step for the real-time propagation is  $\delta t = 0.075$ . The time-dependent propagator  $\hat{U}(t + \delta t, t)$  for the KS Hamiltonian  $\hat{H}_{\text{KS}}(t) = -\frac{\nabla^2}{2} + v_s(\mathbf{r}, t)$  is implemented as follows [39]:

$$\hat{U}(t + \delta t, t) \approx \exp \left\{ -i \frac{\delta t}{2} \hat{H}_{\text{KS}}(t + \delta t) \right\} \exp \left\{ -i \frac{\delta t}{2} \hat{H}_{\text{KS}}(t) \right\}, \quad (9)$$

where  $\hat{H}_{\text{KS}}(t + \delta t)$  is evaluated by using the density coming from the approximately propagated orbitals  $\tilde{\varphi}_j$  according to

$$\tilde{\varphi}_j = \exp\{-i \delta t \hat{H}_{\text{KS}}(t)\} \varphi_j(t). \quad (10)$$

Our simulations always start from the ground state, which is obtained in a self-consistent-field iteration. As mentioned in the introduction, the calculation of probabilities for single ionization, double ionization etc. from the KS orbitals might be questioned since only the density provided by the KS system has rigorous physical meaning. To avoid this problem, we can calculate the total ionization  $N_{\text{ion}}(t) = 1 - N(t)$ , denoting the total number of freed electrons, directly from the density. However, to judge the ionization behaviour for different angular momenta, it is desirable to obtain probabilities also for ionization into states with a hole either in a  $p_-$  or in a  $p_+$  orbital.

To this end, we calculate orbital ionization probabilities  $i_j$  for each KS orbital  $\varphi_j$ . At the end of the propagation time, the probability  $b_j$  to remain bound is approximately calculated by integrating the orbital density over the small region  $|x|, |y| < 5$  a.u. in the same manner as described above for the total number of bound electrons. This leads to raw orbital ionization probabilities  $i'_j = 1 - b_j$ . To improve the accuracy of this calculation, we compute corrected orbital ionization probabilities  $i_j$  as

$$i_j = \frac{i'_j - i'_j(0)}{1 - i'_j(0)}. \quad (11)$$

This accounts for the fact that the box integration yields initial values  $i'_j(0)$  slightly different from zero even though the system starts from the ground state. The correction is relevant only for small applied field strengths that cause only very little ionization. We then obtain the probabilities  $h_-$  and  $h_+$  of finding the system in a singly-charged state with a hole in one of the  $p_+$  orbitals or one of the  $p_-$  orbitals, respectively, while the other orbitals remain bound:

$$h_- = 2i_-(1 - i_-)(1 - i_+)^2, \quad (12)$$

$$h_+ = 2i_+(1 - i_+)(1 - i_-)^2. \quad (13)$$

Here, we have used that the model atom has initially two occupied  $p_-$  and two occupied  $p_+$  orbitals and  $i_-$ ,  $i_+$  denote the ionization probabilities for these orbitals. The ratio of probabilities for generating a singly charged ion with a  $p_-$  hole or a  $p_+$  hole is then evaluated as

$$w = h_-/h_+. \quad (14)$$

This approach essentially identifies the Slater determinant built from the KS orbitals with the physical state. This approximation is made in addition to the use of an approximate exchange-correlation functional, while the calculation of the total ionization does not rely on assigning physical meaning to the KS orbitals. We then compare with the prediction of analytical theory: according to Barth and Smirnova (BS) [18] (see also equations (14),(15) in [19] as well as table 1 therein for the explicit expression and for actual numbers), the ratio  $R$  of ionization rates from the counter-rotating orbital and the co-rotating orbital depends only on the Keldysh parameter

$$\gamma = \frac{\omega}{\mathcal{E}} \sqrt{2I_p}. \quad (15)$$

The BS result was derived under the assumption of constant intensity within a single-electron theory.

In the last part of this paper, we calculate single- and double-ionization probabilities for the ionization of the model atom by double pulses with equal or opposite helicities [21]. In analogy to the ratio  $w$ , this calculation relies on the KS determinant. The ionization probabilities are obtained from the corrected orbital ionization probabilities (11) as

$$p_{\text{single}} = h_- + h_+, \quad (16)$$

$$p_{\text{double}} = i_+^2(1 - i_-)^2 + 4i_-i_+(1 - i_-)(1 - i_+) + i_-^2(1 - i_+)^2. \quad (17)$$

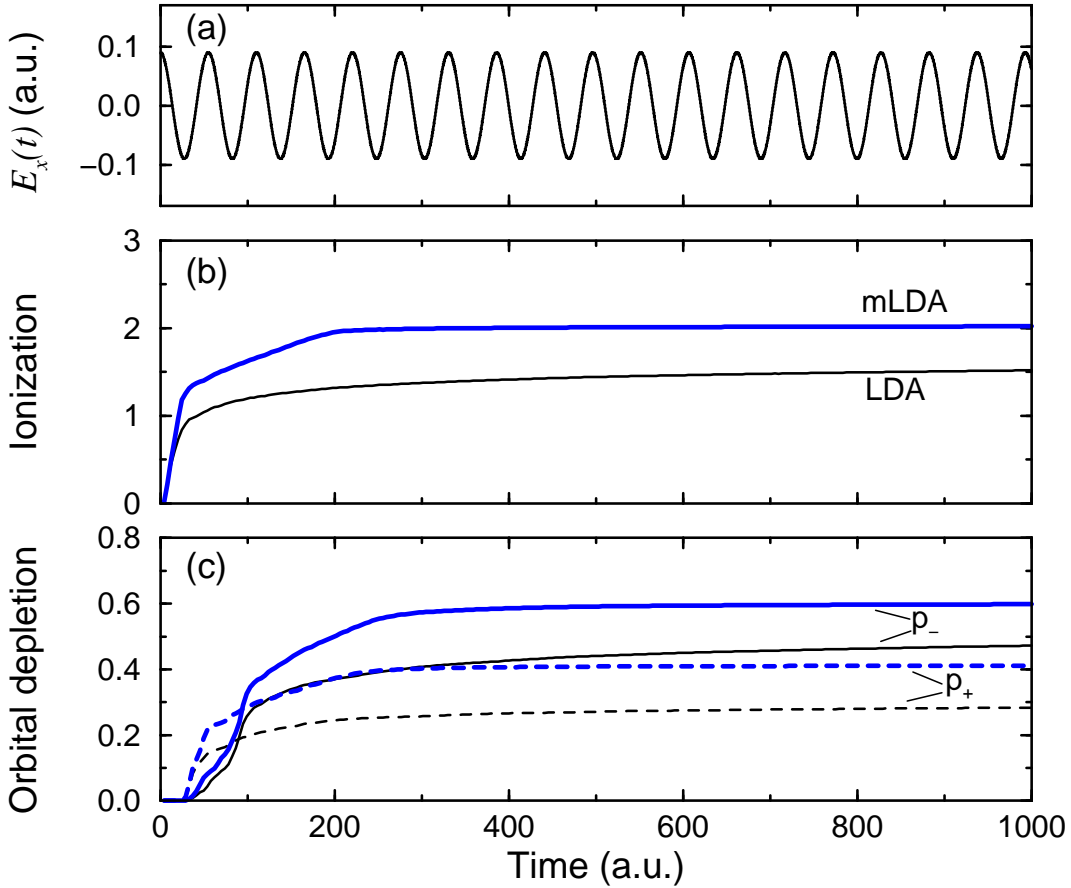


**Figure 2.** Comparison of LDA and mLDA calculations for ionization by a right-circularly polarized 400 nm field of constant field amplitude  $\mathcal{E} = 0.09$ . (a) Time-dependence of the  $x$  component of the circularly polarized electric field. (b) Total ionization from LDA (thin black curve) and mLDA (thick blue curve). (c) Orbital depletion for the  $p_+$  (dashed curves) and  $p_-$  orbitals (solid curves), obtained from LDA (thin black curves) and mLDA (thick blue curves) calculations.

### 3. Results and discussion

First, we investigate the ionization of the atom by a multicycle field in order to demonstrate the difference between the two methods LDA and mLDA. To this end, the atom is subject to a right-circularly polarized field with 400 nm wavelength and constant field amplitude of  $\mathcal{E} = 0.09$ , corresponding to an intensity of  $5.7 \times 10^{14} \text{ W/cm}^2$ . Figure 2 shows the results. Within the shown temporal range, the total ionization reaches values above one. LDA predicts a smooth increase of the total ionization with a severe slowdown of the ionization rate once there is appreciable depletion of the initial state. This is an immediate consequence of the reduced bound-electron charge implying a reduced effect of the repulsive Hartree potential. Importantly, there is no discernible change of this behaviour when the total ionization crosses an integer particle number. In reality, after an electron has been fully removed, further ionization requires overcoming the

higher second ionization energy of the system. The mLDA result shows this behaviour. Between values of one and two of the total ionization, the ionization rate is much smaller than at early times and it slows down much more when the total ionization is near the value two. Interestingly, the calculation somewhat overshoots the value of one before the ionization rate slows down. Most likely this occurs because for the considered field strength, the first ionization step is very fast so that depletion continues before the electron density corresponding to ionization has had time to leave the core region and to cause a change of the correction factor used in mLDA. In figure 2(c), the depletion of the individual orbitals  $p_-$  and  $p_+$  is compared. Here, the depletion is defined as  $D_j(t) = 1 - \int |\varphi_j(\mathbf{r}, t)|^2 d^2r$  where the integration is over the entire grid, whereas for the total ionization in figure 2(b), integration only over the small inner region was used. For this reason, the initial increase at early times in the plotted orbital depletions is slightly later than in the total ionization. The  $s$  orbital is not included in the figure since its depletion is negligible. It is noticeable that the mLDA leads to more depletion than LDA for both orbitals,  $p_-$  and  $p_+$ . Most importantly, we find that in both approaches,  $p_-$  undergoes stronger ionization than  $p_+$ . This is in qualitative accord with the BS predictions [18] and consistent with the previous single-active-electron results for the small-wavelength/low-intensity case [19].

Next, we investigate the ionization by short circularly polarized pulses (three-cycle  $\sin^2$  envelope). The ratio of ionization probabilities into states with a  $p_-$  or  $p_+$  hole is calculated according to Eq. (14). The wavelengths 400 nm, 800 nm and 1600 nm are used in combination with various field strengths. The resulting ratios are plotted as a function of the Keldysh parameter, equation (15), in figure 3. One important point to note here is that the Keldysh parameter is evaluated using the first ionization potential of the neutral atom although in the TDDFT simulation, higher charge states can be reached depending on the field intensity. We return to this issue below. For comparison, the analytical BS result [18] is also shown in the figure. Overall the TDDFT results are in good agreement with the single-electron theory. We notice that mLDA produces somewhat lower ratios than LDA so that the agreement with BS improves at small wavelength and worsens at long wavelength. In the numerical single-electron calculations, see figure 1 in [19], the ratios are slightly below the BS ratio for almost all laser parameters except small field strengths. This suggests that the present mLDA results, which are mostly below the BS ratios as well, are more trustworthy than the LDA results. In the 800 nm data, we observe that the TDDFT ratio is slightly above the BS ratio for very low Keldysh parameter. This finding differs from the single-electron result in [19], where the ratio at low Keldysh parameter falls even below the value one. The behaviour of TDDFT can be explained by inspection of the total ionization at the various laser parameters, see the insets in figure 3. For the leftmost points of the 800 nm data, the total ionization is substantially above one (1.96 and 1.29) in the mLDA calculation. This means that for these few points it is not quite appropriate to consider just the first ionization potential for evaluation of the Keldysh parameter. Effectively, the increased ionization potential of higher charge states implies a higher Keldysh parameter and thus to an increased

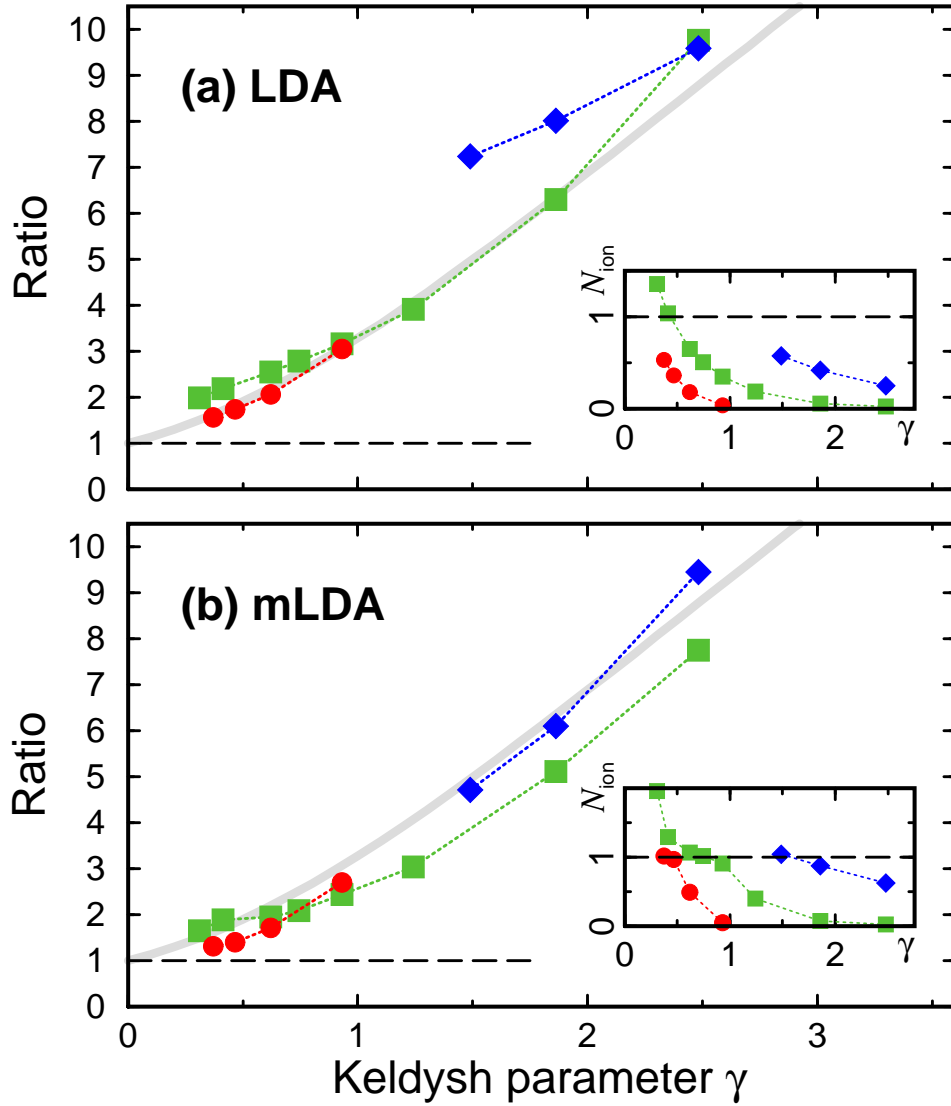


**Figure 3.** Ratio of probabilities for generating a singly-charged ion with a hole either in a  $p_-$  orbital or in a  $p_+$  orbital by ionization with a three-cycle right-circular pulse with wavelength 1600nm (red circles), 800nm (green squares) or 400nm (blue diamonds) at various field intensities. (a) LDA results, (b) mLDA results. The thick grey curves give the prediction by Barth and Smirnova [18] for the ratio of ionization rates. The Keldysh parameter  $\gamma$  is evaluated using the ionization potential of the neutral atom. The insets show the total ionization (number of freed electrons) as a function of the Keldysh parameter.

ratio  $w$  according to the BS theory. For the other laser parameters used in figure 3, the total ionization is around or less than one so that using the first ionization potential is appropriate. Closer inspection of the total ionization from the mLDA calculation in the inset of figure 3(b) shows a step-like at the Keldysh parameter where the number of freed electrons  $N_{\text{ion}}$  is close to 1. This is a consequence of the mLDA construction, which enforces a rapid change of the KS potential when passing through integer  $N_{\text{ion}}$ .

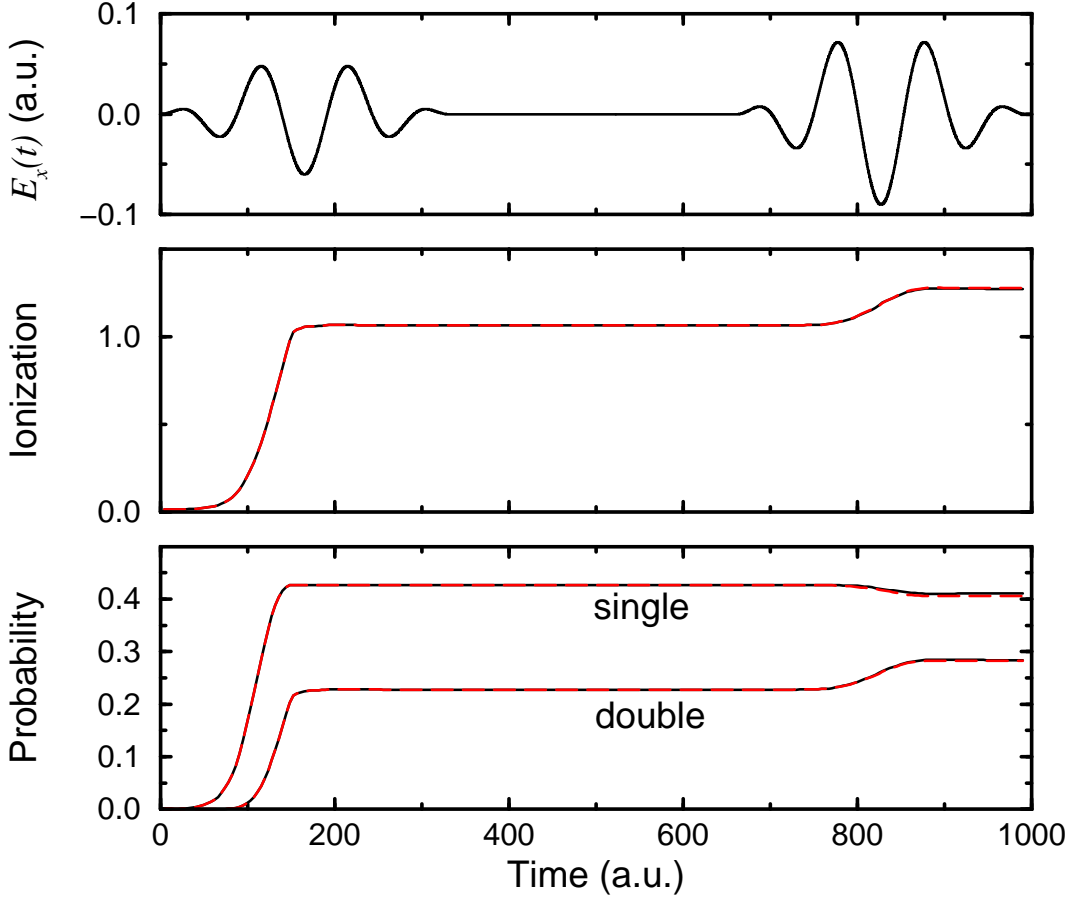


**Figure 4.** Ionization of the model atom by a two-pulse sequence with equal (right-right) or opposite (right-left) helicities using mLDA TDDFT simulations. The pulses are three-cycle 800 nm pulses with field amplitudes 0.06 a.u. and 0.09 a.u., respectively. (a) Time dependence of the  $x$  component of the electric field. (b) Total ionization from equal helicities (solid black curve) and opposite helicities (red dashed curve). (c) Single- and double-ionization probabilities from equal helicities (solid black curves) and opposite helicities (red dashed curves).

The LDA results in the inset of figure 3(a) are instead smooth curves without a step.

Ideally, one would like to use TDDFT to successfully describe genuine multielectron effects such as double ionization. Inspired by the experiment of Herath et al. [21] we simulate the ionization of the model atom by a sequence of two circularly polarized pulses, either with equal or opposite sense of rotation of the electric field. According to experiment and theory [21, 22] for ionization of argon atoms, the yield of doubly-charged ions is much higher for opposite helicities because in this case the two pulses are able to deplete opposite  $m$  quantum numbers. Unfortunately, the TDDFT results (figure 4) do not show any sign of this effect. In fact, the time dependence of the total ionization in figure 4(b) and the single- and double-ionization probabilities in figure 4(c) are practically the same for both field configurations. They can hardly be distinguished on the scale of the graph. We have obtained similar results also for other laser parameters

(not shown). Most likely, the difference to [21, 22] arises because the  $\text{Ar}^{2+}$  ion has a  $^3P$  ground state which is not compatible with removing two electrons with the same magnetic quantum number  $m$  from the neutral atom, while the KS determinant after ionization naturally includes such contributions. It then seems that the interpretation of the KS determinant as a physical state can lead to unsatisfactory results. More work will be needed to construct a proper density functional for double-ionization probabilities.

#### 4. Conclusion

Ionization of multielectron systems by circularly polarized laser pulses is a highly important topic in current femtosecond and attosecond research. Our work suggests that time-dependent density functional theory can be successfully applied to such problems if standard schemes such as the local density approximation are modified to respect the particle number discontinuity. Our TDDFT results show that angular momentum orbitals with electrons rotating against the applied field are ionized more easily than corotating orbitals, in analogy to previous results from single-electron calculations. The correct prediction of multiple-ionization probabilities within TDDFT, however, will require more theory development in the future.

#### Acknowledgments

We thank Ingo Barth for useful discussions.

#### References

- [1] Calegari F, Sansone G, Stagira S, Vozzi C and Nisoli M 2016 *J. Phys. B: At. Mol. Opt. Phys.* **49** 062001 URL <http://stacks.iop.org/0953-4075/49/i=6/a=062001>
- [2] Staudte A, Patchkovskii S, Pavičić D, Akagi H, Smirnova O, Zeidler D, Meckel M, Villeneuve D M, Dörner R, Ivanov M Y and Corkum P B 2009 *Phys. Rev. Lett.* **102** 033004 URL <http://link.aps.org/doi/10.1103/PhysRevLett.102.033004>
- [3] Holmegaard L, Hansen J L, Kalthøj L, Louise Kragh S, Stapelfeldt H, Filsinger F, Küpper J, Meijer G, Dimitrovski D, Abu-samha M, Martiny C P J and Bojer Madsen L 2010 *Nat. Phys.* **6** 428–432 URL <http://dx.doi.org/10.1038/nphys1666>
- [4] Zhu X, Zhang Q, Hong W, Lu P and Xu Z 2011 *Opt. Express* **19** 13722–13731 URL <http://www.opticsexpress.org/abstract.cfm?URI=oe-19-15-13722>
- [5] Spanner M, Gräfe S, Chelkowski S, Pavičić D, Meckel M, Zeidler D, Bardon A B, Ulrich B, Bandrauk A D, Villeneuve D M, Dörner R, Corkum P B and Staudte A 2012 *J. Phys. B: At. Mol. Opt. Phys.* **45** 194011 URL <http://stacks.iop.org/0953-4075/45/i=19/a=194011>

- [6] Petersen I, Henkel J and Lein M 2015 *Phys. Rev. Lett.* **114** 103004 URL <http://link.aps.org/doi/10.1103/PhysRevLett.114.103004>
- [7] Eckle P, Smolarski M, Schlup P, Biegert J, Staudte A, Schöffler M, Muller H G, Dörner R and Keller U 2008 *Nat. Phys.* **4** 565–570 URL <http://dx.doi.org/10.1038/nphys982>
- [8] Pfeiffer A N, Cirelli C, Smolarski M, Dimitrovski D, Abu-samha M, Madsen L B and Keller U 2012 *Nat. Phys.* **8** 76–80 URL <http://dx.doi.org/10.1038/nphys2125>
- [9] Torlina L, Morales F, Kaushal J, Ivanov I, Kheifets A, Zielinski A, Scrinzi A, Muller H G, Sukiasyan S, Ivanov M and Smirnova O 2015 *Nat. Phys.* **11** 503–508 URL <http://dx.doi.org/10.1038/nphys3340>
- [10] Lux C, Wollenhaupt M, Bolze T, Liang Q, Köhler J, Sarpe C and Baumert T 2012 *Angewandte Chemie International Edition* **51** 5001–5005 URL <http://dx.doi.org/10.1002/anie.201109035>
- [11] Lehmann C S, Ram N B, Powis I and Janssen M H M 2013 *J. Chem. Phys.* **139** 234307 URL <http://scitation.aip.org/content/aip/journal/jcp/139/23/10.1063/1.4844295>
- [12] Dreissigacker I and Lein M 2014 *Phys. Rev. A* **89** 053406 URL <http://link.aps.org/doi/10.1103/PhysRevA.89.053406>
- [13] Lux C, Wollenhaupt M, Sarpe C and Baumert T 2015 *ChemPhysChem* **16** 115–137 URL <http://dx.doi.org/10.1002/cphc.201402643>
- [14] Lux C, Senftleben A, Sarpe C, Wollenhaupt M and Baumert T 2016 *J. Phys. B: At. Mol. Opt. Phys.* **49** 02LT01 URL <http://stacks.iop.org/0953-4075/49/i=2/a=02LT01>
- [15] Beaulieu S, Ferré A, Gneaux R, Canonge R, Descamps D, Fabre B, Fedorov N, Légaré F, Petit S, Ruchon T, Blanchet V, Mairesse Y and Pons B 2016 *New J. Phys.* **18** 102002 URL <http://stacks.iop.org/1367-2630/18/i=10/a=102002>
- [16] Popruzhenko S V 2014 *J. Phys. B: At. Mol. Opt. Phys.* **47** 204001 URL <http://stacks.iop.org/0953-4075/47/i=20/a=204001>
- [17] Beiser S, Klaiber M and Kiyan I Y 2004 *Phys. Rev. A* **70** 011402 URL <http://link.aps.org/doi/10.1103/PhysRevA.70.011402>
- [18] Barth I and Smirnova O 2013 *Phys. Rev. A* **87** 013433 URL <http://link.aps.org/doi/10.1103/PhysRevA.87.013433>
- [19] Barth I and Lein M 2014 *J. Phys. B: At. Mol. Opt. Phys.* **47** 204016 URL <http://stacks.iop.org/0953-4075/47/i=20/a=204016>
- [20] Mauger F and Bandrauk A D 2014 *J. Phys. B: At. Mol. Opt. Phys.* **47** 191001 URL <http://stacks.iop.org/0953-4075/47/i=19/a=191001>
- [21] Herath T, Yan L, Lee S K and Li W 2012 *Phys. Rev. Lett.* **109** 043004 URL <http://link.aps.org/doi/10.1103/PhysRevLett.109.043004>
- [22] Barth I and Smirnova O 2013 *Phys. Rev. A* **87** 065401 URL <http://link.aps.org/doi/10.1103/PhysRevA.87.065401>

- [23] Taylor K T, Parker J S, Dundas D and Meharg K J 2007 *J. Mod. Opt.* **54** 1959–1983 URL <http://dx.doi.org/10.1080/09500340701483154>
- [24] Ruiz C, Plaja L and Roso L 2005 *Phys. Rev. Lett.* **94** 063002 URL <http://link.aps.org/doi/10.1103/PhysRevLett.94.063002>
- [25] Runge E and Gross E K U 1984 *Phys. Rev. Lett.* **52**(12) 997–1000 URL <http://link.aps.org/doi/10.1103/PhysRevLett.52.997>
- [26] Ullrich C A 2012 *Time-Dependent Density-Functional Theory: Concepts and Applications (Oxford Graduate Texts)* (Oxford: Oxford University Press)
- [27] Fittinghoff D N, Bolton P R, Chang B and Kulander K C 1992 *Phys. Rev. Lett.* **69** 2642–2645 URL <http://link.aps.org/doi/10.1103/PhysRevLett.69.2642>
- [28] Walker B, Sheehy B, DiMauro L F, Agostini P, Schafer K J and Kulander K C 1994 *Phys. Rev. Lett.* **73** 1227–1230 URL <http://link.aps.org/doi/10.1103/PhysRevLett.73.1227>
- [29] Bauer D 1997 *Phys. Rev. A* **56** 3028–3039 URL <http://link.aps.org/doi/10.1103/PhysRevA.56.3028>
- [30] Lappas D G and van Leeuwen R 1998 *J. Phys. B: At. Mol. Opt. Phys.* **31** L249–256 URL <http://stacks.iop.org/0953-4075/31/i=6/a=001>
- [31] Petersilka M and Gross E K U 1999 *Laser Physics* **9** 105
- [32] Lein M and Kümmel S 2005 *Phys. Rev. Lett.* **94** 143003 URL <http://link.aps.org/doi/10.1103/PhysRevLett.94.143003>
- [33] Perdew J P, Parr R G, Levy M and Balduz J L 1982 *Phys. Rev. Lett.* **49** 1691–1694 URL <http://link.aps.org/doi/10.1103/PhysRevLett.49.1691>
- [34] de Wijn A S, Lein M and Kümmel S 2008 *Europhys. Lett.* **84** 43001 URL <http://stacks.iop.org/0295-5075/84/i=4/a=43001>
- [35] Thiele M, Gross E K U and Kümmel S 2008 *Phys. Rev. Lett.* **100** 153004 URL <http://link.aps.org/doi/10.1103/PhysRevLett.100.153004>
- [36] Dreissigacker I and Lein M 2011 *Chem. Phys.* **391** 143 – 146 URL <http://www.sciencedirect.com/science/article/pii/S0301010411000528>
- [37] Wilken F and Bauer D 2006 *Phys. Rev. Lett.* **97** 203001 URL <http://link.aps.org/doi/10.1103/PhysRevLett.97.203001>
- [38] Attaccalite C, Moroni S, Gori-Giorgi P and Bachelet G B 2002 *Phys. Rev. Lett.* **88** 256601 URL <http://link.aps.org/doi/10.1103/PhysRevLett.88.256601>
- [39] Castro A, Rubio A, Strubbe D, Nogueira F, Marques M and Oliveira M 2012 *Guided Construction of a 2D TDDFT code* presented at 5th International Workshop and School on Time-Dependent Density-Functional Theory: Prospects and Applications, Benasque URL <http://stacks.iop.org/0953-4075/49/i=2/a=02LT01>